ARTICLE IN PRESS

Available online at www.sciencedirect.com

ScienceDirect

Journal of the Franklin Institute ▮ (▮▮▮▮) ▮▮▮–▮▮▮

Journal of The Franklin Institute

www.elsevier.com/locate/jfranklin

A novel disturbance observer-based backstepping controller with command filtered compensation for a MIMO system

Ramy Rashad[a], Ahmed Aboudonia[a], Ayman El-Badawy[b,*]

[a]Mechatronics Department, Faculty of Engineering and Materials Science, German University in Cairo, Cairo, Egypt
[b]Mechanical Engineering Department, Al-Azhar University and German University in Cairo, Cairo, Egypt

Received 26 September 2015; received in revised form 14 June 2016; accepted 28 July 2016

Abstract

This paper presents a novel disturbance observer-based trajectory tracking controller based on the integral backstepping approach. To avoid the complexity of analytically calculating derivatives of virtual control signals in the standard backstepping technique, a command filtered backstepping approach is utilized. The proposed control approach is formulated for a class of nonlinear MIMO systems and provides robustness against external disturbances. This approach is applied on an aerodynamic laboratory setup known as the twin rotor MIMO system (TRMS). Stability analysis of the proposed controller is presented using Lyapunov stability arguments and singular perturbation theory. Simulation studies show that the proposed controller successfully allows the system outputs to track arbitrary reference trajectories and reject arbitrary constant disturbances that may occur due to partial actuator failure. The reliability and effectiveness of the approach is validated experimentally by implementation of the proposed controller on a hardware-in-the-loop system.

1. Introduction

In nonlinear control systems, Lyapunov's method is one of the most useful tools in feedback design. In many control techniques, the boundedness of trajectories and error convergence

*Corresponding author.
E-mail addresses: ramy.abdelmonem@guc.edu.eg (R. Rashad), ahmed.abou-donia@guc.edu.eg (A. Aboudonia), ayman.elbadawy@guc.edu.eg (A. El-Badawy).

http://dx.doi.org/10.1016/j.jfranklin.2016.07.017
0016-0032/

Please cite this article as: R. Rashad, et al., A novel disturbance observer-based backstepping controller with command filtered compensation for a MIMO system, Journal of the Franklin Institute. (2016), http://dx.doi.org/10.1016/j.jfranklin.2016.07.017

properties are guaranteed based on designing the control laws such that the derivative of a Lyapunov function has specific properties. Combined with other tools such as LaSalle's principles or Barbalat's Lemma, many nonlinear control techniques have been introduced in the previous decades. One of these techniques is the backstepping control approach which is a recursive design procedure that breaks down the control design for the full system into a sequence of lower-order subsystems. One of the main advantages of the backstepping technique is its flexibility in designing stabilizing and tracking controllers under less restrictive conditions than other techniques [1]. In addition, the backstepping technique permits the exploitation of useful nonlinearities in the system unlike the feedback linearization technique which cancels all nonlinearities thus requiring precise mathematical models [2].

A major limitation in the standard backstepping technique is its lack of robustness against external disturbances. One way of robustifying the backstepping technique is by augmenting it with integral control. In [3], different methods have been analyzed on the augmentation of integral control with the backstepping technique. In theory, integral control can eliminate constant steady state offsets. However, in the presence of time-varying disturbances, the integral action might cause undesirable transient performances in addition to a steady state tracking error. A more elaborate discussion on integral control has been introduced in [4], which classifies integral control as a passive anti-disturbance control method. A more effective way to handle disturbances and improve robustness of the closed loop system is through disturbance observer-based (DOB) control. DOB control can handle disturbances through a faster dynamic response compared to integral control [4]. The reason behind such performance is that DOB approaches include feedforward compensation that directly combat the disturbances in the system. In addition, DOB control approaches can preserve the nominal performance of the baseline controller in the absence of disturbances unlike most of the existing robust control methods [4]. In the literature, several applications have exploited the combination of backstepping and disturbance observers. Applications include control of a magnetic levitation system [5], guidance and control of missiles [6] and robotic manipulators [7].

Another limitation of the standard backstepping technique is the requirement of computing derivatives of command signals at each step of the design. As the order of the system increases, analytically computing the command signals derivative would be very tedious. In addition, the direct differentiation of these command signals might be impractical in applications as it would amplify the high-frequency noise contained in these signals. Even if the exact analytical expressions of the command signal derivatives can be computed, it would be based on the nominal model of the plant which requires a high fidelity mathematical model. In recent years, a practical extension of the standard backstepping technique was introduced, which is known as command filtered backstepping [8]. The main idea of the command filtered backstepping approach is that the command derivatives are generated using low pass filters and then the backstepping variables are extended to retain the stability of the closed loop system. Hence, the analytical derivation or direct differentiation of the command signals derivatives will be eliminated. However, a main limitation of the proposed scheme in [8] is the lack of robustness to external disturbances applied to the system.

In this study, we propose a novel nonlinear controller which combines the integral backstepping technique, disturbance observers and the command filtering extension. The controller is formulated for a class of square and affine nonlinear systems which can be written in strict feedback form. This class of systems represents several fully actuated m-degrees-of-freedom (m-DOF) mechanical systems. Examples of such systems include m-DOF robotic manipulators and 6-DOF underwater vehicles. A disturbance observer is augmented to the

Please cite this article as: R. Rashad, et al., A novel disturbance observer-based backstepping controller with command filtered compensation for a MIMO system, Journal of the Franklin Institute. (2016), http://dx.doi.org/10.1016/j.jfranklin.2016.07.017

backstepping-based controller to estimate disturbances in the system model. These disturbances can be due to constant external sources, unmodeled dynamics or modeled dynamics that are intentionally neglected such that the system model can be written in strict feedback form. Thus, the proposed approach is applicable to a wider class of systems that can be written in strict feedback form by neglecting certain parts of the dynamics that cause cross-coupling. To counteract the disturbance estimation error, integral action is utilized to eliminate this error. Finally, the approach computes the command signal derivatives using low pass filters. The benefits of the presented control approach include: (1) retaining the advantages of the standard backstepping technique which provides the designer with a systematic, decoupled and flexible design methodology; (2) providing the system with active disturbance rejection properties, thus avoiding the drawbacks of integral control which would have risen if it was used alone to reject time varying disturbances; and, (3) eliminating the complexity of deriving the command signals analytically or differentiating them through the use of command filters. The detailed stability analysis of the overall closed loop system is presented based on singular perturbation theory and Lyapunov stability arguments. This analysis will take into consideration the effects of the disturbance estimation errors and the errors due to the command filters. It is worth mentioning that a simpler version of this control scheme has been previously applied in [9] on an autonomous aerial vehicle. However, it neither included a disturbance observer nor the formal stability analysis presented herein.

To validate the proposed approach, it is applied on an aerodynamical experimental setup known as the twin rotor MIMO system (TRMS). The TRMS is a laboratory setup which resembles a helicopter prototype designed for flight control experiments as shown in Fig. 1. The control system design of the TRMS is challenging since its mathematical model is a high order nonlinear system with heavy cross-coupling effects between the two propellers [10]. In the literature, several research studies have been carried out for to design control systems for the TRMS test bed. Fuzzy logic control has been used for the design of tracking controllers in several studies as in [11–14] which included also experimental validation of the presented controllers. Moreover, sliding mode control (SMC) has been utilized for the control of the TRMS to increase the robustness of the system to parametric uncertainties and external disturbances such as [10,15,16]. In this study, the TRMS model is formulated in strict feedback form by neglecting parts of the system dynamics that cause cross-coupling in the equations. The advantage of controlling the system using the backstepping technique is that the natural time-scale separation between the TRMS dynamics and its actuator dynamics is exploited in the design process. The proposed controller is implemented in simulation and its effectiveness is tested through several simulation scenarios. These scenarios include tracking pre-specified

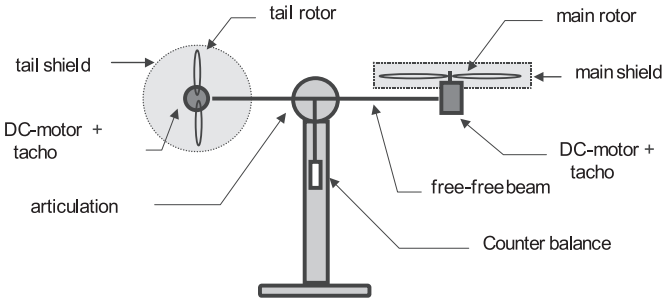

Fig. 1. TRMS Schematic diagram [17].

Please cite this article as: R. Rashad, et al., A novel disturbance observer-based backstepping controller with command filtered compensation for a MIMO system, Journal of the Franklin Institute. (2016), http://dx.doi.org/10.1016/j.jfranklin.2016.07.017

trajectories in addition to stabilization of the system's outputs in the presence of disturbances due to partial actuator failure. Finally, experimental validation of the proposed controller on a laboratory setup through a hardware-in-the-loop system is carried out and the results are presented and discussed.

2. Problem formulation

Consider the following class of n-th order square affine MIMO systems in strict feedback form. Systems in this form represent a class of fully actuated m-degrees-of-freedom mechanical systems. Without loss of generality, the state vector $\boldsymbol{x}$, is assumed to be divided into three groups $\boldsymbol{x} = [x_1^\top, x_2^\top, x_3^\top]^\top \in \mathbb{R}^n$ such that $x_i \in \mathbb{R}^{n_i}$ and $\sum_{i=1}^{3} n_i = n$. Although this article considers this case, the results can be easily extended to general cases where the state vector is divided into more than three groups. The state space equations of the systems considered are given by

$$\begin{aligned}
\dot{x}_1 &= f_1(x_1) + g_1(x_1)x_2 + d_1, \quad x_1(0) = x_{10} \\
\dot{x}_2 &= f_2(x_1, x_2) + g_2(x_1, x_2)x_3 + d_2, \quad x_2(0) = x_{20} \\
\dot{x}_3 &= f_3(x_1, x_2, x_3) + g_3(x_1, x_2, x_3)u + d_3, \quad x_3(0) = x_{30} \\
y &= x_1,
\end{aligned} \tag{1}$$

where $u, y \in \mathbb{R}^m$ are the input and output vectors, while f_i and g_i are nonlinear smooth vector fields. The first state vector x_1 is considered as the system's output (i.e., $m = n_1$). The terms $d_i \in \mathbb{R}^{n_i}$ include external disturbances, unmodeled dynamics, and modeled dynamics intentionally neglected such that the original system model can be written in strict feedback form. The functions f_i and g_i are assumed to be known and their continuity properties are stated below in Assumption 1. Moreover, Assumption 2, which is standard in vector backstepping, will be invoked to ensure controllability. This implies that the system (1) cannot possess any empty groups as this will lead to an uncontrollable system.

The control objective to be addressed is the design of a continuous control law $u(t)$ such that the output $y(t) = x_1(t)$ tracks a desired output trajectory $x_d(t) \in \mathbb{R}^{n_1}$ from any initial conditions, within a guaranteed precision ϵ, in the presence of the time-varying disturbances d_i. In addition, the control signal should ensure the boundedness of the remaining states (x_2 and x_3). The desired trajectory $x_d(t)$ and the disturbances $d_i(t)$ are required to satisfy Assumptions 3 and 4 respectively.

Assumption 1. For each $i = \{1, 2, 3\}$, all elements of f_i and g_i and their first partial derivatives are continuous and bounded on any compact set $\mathcal{D}_i \subset \mathbb{R}^k$, where $k = \sum_{j=1}^{i} n_j$.

Assumption 2. There exists a constant $g_0 > 0$ such that the determinant of each matrix $|det(g_i(\cdot))| \geq g_0$.

Assumption 3. For $t \geq 0$, the signal $x_d(t)$ and its time derivative $\dot{x}_d(t)$ are both continuous, bounded and available.

Assumption 4. For $t \geq 0$, the disturbance signals $d_i(t)$ are continuous and norm bounded, i.e. $\| d_i(t) \| < \eta_i$ where η_i are positive constants

Please cite this article as: R. Rashad, et al., A novel disturbance observer-based backstepping controller with command filtered compensation for a MIMO system, Journal of the Franklin Institute. (2016), http://dx.doi.org/10.1016/j.jfranklin.2016.07.017

3. Control system design

This section presents the DOB integral backstepping control approach with command filtering. The control system design is divided into three steps in Sections 3.1–3.3, one for each subsystem in Eq. (1). The first step considers stabilizing the tracking error $(x_d - x_1)$ while the command filtering extension is performed in the second and third steps. In each step a nonlinear disturbance observer will be designed to provide an estimate $\hat{d}_i \in \mathbb{R}^{n_i}$ of the actual disturbance d_i. In addition, an integrator is added in each step to combat the disturbance estimation error. The properties of the presented approach and its stability proof, based on singular perturbation theory, will be presented in Section 4.

3.1. Controller design step 1

The first step of the controller design considers the virtual subsystem

$$\dot{x}_1 = f_1 + g_1 v_1 + d_1, \tag{2}$$

where $v_1 \in \mathbb{R}^{n_2}$ is the virtual input to be designed. Then we define the following two backstepping variables

$$z_1 = x_d - x_1, \quad \xi_1 = \int_0^t z_1(\tau)d\tau, \quad \xi_1(0) = 0, \tag{3}$$

where $z_1, \xi_1 \in \mathbb{R}^{n_1}$ represent the tracking error and its integration respectively. We then proceed by choosing the following quadratic Lyapunov function

$$V_1 = \tfrac{1}{2} z_1^\top z_1 + \tfrac{1}{2}\xi_1^\top \Lambda_1 \xi_1, \tag{4}$$

where $\Lambda_1 = \Lambda_1^\top \in \mathbb{R}^{n_1 \times n_1}$ is a diagonal positive definite gain matrix. The time derivative of V_1 along the trajectories of the system (2) is given by

$$\begin{aligned} \dot{V}_1 &= z_1^\top \dot{z}_1 + \xi_1^\top \Lambda_1 \dot{\xi}_1 \\ &= z_1^\top (\dot{x}_d - \dot{x}_1) + \xi_1^\top \Lambda_1 z_1 \\ &= z_1^\top (\dot{x}_d - f_1 - g_1 v_1 - d_1 + \Lambda_1 \xi_1). \end{aligned} \tag{5}$$

Before proceeding with the design of the control law v_1, the disturbance observer responsible for estimating d_1 will be designed. An estimate $\hat{d}_1$ of the disturbance vector can be generated using a basic disturbance observer suggested in [18] as

$$\dot{\hat{d}}_1 = -\mu_1 \hat{d}_1 + \mu_1(\dot{x}_1 - f_1 - g_1 v_1), \tag{6}$$

where $\mu_1 > 0$ is a positive constant representing the observer gain. A requirement for such an observer is the availability of the output's derivative $\dot{x}_1$ which may be unpractical in real applications. An enhanced formulation of the disturbance observer, introduced in [18], for computing the disturbance estimate $\hat{d}_1$ is depicted by

$$\dot{\delta}_1 = -\mu_1 \delta_1 - \mu_1^2 x_1 - \mu_1(f_1 + g_1 v_1), \quad \delta_1(0) = -\mu_1 x_{10}, \tag{7}$$

$$\hat{d}_1 = \delta_1 + \mu_1 x_1, \tag{8}$$

where $\delta_1 \in \mathbb{R}^{n_1}$ is an internal variable of the observer. The disturbance estimation error e_{d_1} and its associated dynamics are given by [18]

Please cite this article as: R. Rashad, et al., A novel disturbance observer-based backstepping controller with command filtered compensation for a MIMO system, Journal of the Franklin Institute. (2016), http://dx.doi.org/10.1016/j.jfranklin.2016.07.017

$$e_{d_1} = \hat{d}_1 - d_1 \tag{9}$$

$$\dot{e}_{d_1} = -\mu_1 e_{d_1} - \dot{d}_1, \quad e_{d_1}(0) = -d_{10}, \tag{10}$$

where $d_{10} = d_1(0)$. It can be easily observed that the error dynamics (10) represents a set of n_1 decoupled first order systems. In the case of a constant disturbance (i.e., $\dot{d}_1 = 0$), the error e_{d_1} asymptotically converges to zero where μ_1 controls the rate of convergence. This can be easily observed since the error dynamics (10) is linear and μ_1 is a positive constant. Furthermore, in the case of a time-varying disturbance, the bounded-input bounded-output stability of the error dynamics is guaranteed [19, p. 125] due to Assumption 4. The effect of this bounded error on the overall closed loop system will be discussed in the coming section.

Now returning to Eq. (5), the virtual control input is chosen to be

$$\upsilon_1 = g_1^{-1}(\Lambda_1 \xi_1 + \dot{x}_d - f_1 - \hat{d}_1 + A_1 z_1), \tag{11}$$

where $A_1 = A_1^\top \in \mathbb{R}^{n_1 \times n_1}$ is a diagonal positive definite matrix. Moreover, with Assumption 2 the matrix g_1 is guaranteed to be non-singular for all x_1. Hence, by choosing υ_1 as Eq. (11) and neglecting the disturbance estimation error, Eq. (5) can be written as

$$\begin{aligned} \dot{V}_1 &= z_1^\top (-A_1 z_1 + \hat{d}_1 - d_1) \\ &= -z_1^\top A_1 z_1, \quad \forall z_1 \neq 0. \end{aligned} \tag{12}$$

This concludes the first stage of the controller design. The detailed stability analysis of the closed loop system will be discussed in a subsequent section of the article.

3.2. Controller design step 2

The second step in the controller design considers the virtual subsystem given by

$$\dot{x}_2 = f_2 + g_2 \upsilon_2 + d_2, \tag{13}$$

where $\upsilon_2 \in \mathbb{R}^{n_3}$ is the second virtual input. The next backstepping variables are chosen to be

$$z_2 = \upsilon_{1,f} - x_2, \quad \xi_2 = \int_0^t z_2(\tau) d\tau, \quad \xi_2(0) = 0, \tag{14}$$

where $\upsilon_{1,f} \in \mathbb{R}^{n_2}$ represents the filtered command signal generated using the first order low pass filter

$$\dot{\upsilon}_{1,f} = \gamma(\upsilon_1 - \upsilon_{1,f}), \quad \upsilon_{1,f}(0) = \upsilon_{10}, \tag{15}$$

where $\gamma > 0$ is a positive constant that represents the filter's cut-off frequency. Whereas $\upsilon_{10} = \upsilon_1(x_{10}, x_{d0}, \dot{x}_{d0})$ denotes the initial value of the virtual control signal (11), with $x_{d0} = x_d(0)$ and $\dot{x}_{d0} = \dot{x}_d(0)$.

The time derivative of the first backstepping variable along the trajectories of the system (1) can be written as

$$\dot{z}_1 = \dot{x}_d - \dot{x}_1 = \dot{x}_d - f_1 - g_1 x_2 - d_1. \tag{16}$$

By adding and subtracting the terms υ_1 and $\upsilon_{1,f}$ from x_2, the previous equation can be written as

$$\dot{z}_1 = \dot{x}_d - f_1 - g_1(x_2 + \upsilon_1 - \upsilon_1 + \upsilon_{1,f} - \upsilon_{1,f}) - d_1. \tag{17}$$

By rearranging the terms of Eq. (17), it can be written as

$$\dot{z}_1 = \dot{x}_d - f_1 - d_1 - g_1 \upsilon_1 + g_1(\upsilon_{1,f} - x_2) + g_1(\upsilon_1 - \upsilon_{1,f}). \tag{18}$$

Please cite this article as: R. Rashad, et al., A novel disturbance observer-based backstepping controller with command filtered compensation for a MIMO system, Journal of the Franklin Institute. (2016), http://dx.doi.org/10.1016/j.jfranklin.2016.07.017

By using Eqs. (9), (11), (14), and after some simplification, $\dot{z}_1$ becomes

$$\dot{z}_1 = -A_1 z_1 - \Lambda_1 \xi_1 + e_{d_1} + g_1 z_2 + g_1(v_1 - v_{1,f}), \tag{19}$$

where the last occurrence of v_1 in Eq. (18) was deliberately not replaced by Eq. (11).

To compensate the influence of the command filter on the closed loop stability, a new vector $\varepsilon_1 \in \mathbb{R}^{n_1}$ is introduced such that the compensated tracking error signal and its integration are defined as

$$\overline{z}_1 = z_1 - \varepsilon_1, \quad \overline{\xi}_1 = \int_0^t \overline{z}_1(\tau)d\tau = \xi_1 - \chi_1, \tag{20}$$

where $\chi_1 = \int_0^t \varepsilon_1(\tau)d\tau$. We then proceed by choosing the augmented Lyapunov function

$$V_2 = \tfrac{1}{2}\overline{z}_1^\top \overline{z}_1 + \tfrac{1}{2}\overline{\xi}_1^\top \Lambda_1 \overline{\xi}_1 + \tfrac{1}{2} z_2^\top z_2 + \tfrac{1}{2}\xi_2^\top \Lambda_2 \xi_2, \tag{21}$$

where $\Lambda_2 = \Lambda_2^\top \in \mathbb{R}^{n_2 \times n_2}$ is a diagonal positive definite matrix. The time derivative of V_2 is given by

$$\begin{aligned} \dot{V}_2 &= \overline{z}_1^\top \dot{\overline{z}}_1 + \overline{\xi}_1^\top \Lambda_1 \dot{\overline{\xi}}_1 + z_2^\top \dot{z}_2 + \xi_2^\top \Lambda_2 \dot{\xi}_2 \\ &= \overline{z}_1^\top (\dot{z}_1 - \dot{\varepsilon}_1) + \overline{\xi}_1^\top \Lambda_1 \overline{z}_1 + z_2^\top (\dot{v}_{1,f} - \dot{x}_2) + \xi_2^\top \Lambda_2 z_2 \end{aligned} \tag{22}$$

Evaluating the previous equation along the trajectories of the system (13) and using Eqs. (19)–(20) yields

$$\begin{aligned} \dot{V}_2 &= \overline{z}_1^\top (\dot{z}_1 - \dot{\varepsilon}_1) + \overline{\xi}_1^\top \Lambda_1 \overline{z}_1 + z_2^\top (\dot{v}_{1,f} - \dot{x}_2) + \xi_2^\top \Lambda_2 z_2 \\ &= \overline{z}_1^\top [-A_1 z_1 - \Lambda_1 \xi_1 + e_{d_1} + g_1 z_2 + g_1(v_1 - v_{1,f}) - \dot{\varepsilon}_1 + \Lambda_1^\top (\xi_1 - \chi_1)] \\ &\quad + z_2^\top (\dot{v}_{1,f} - f_2 - g_2 v_2 - d_2 + \Lambda_2^\top \xi_2) \\ &= \overline{z}_1^\top (-A_1 z_1 - \Lambda_1 \chi_1 + g_1(v_1 - v_{1,f}) - \dot{\varepsilon}_1) + z_2^\top (g_1^\top \overline{z}_1 + \dot{v}_{1,f} - f_2 - g_2 v_2 - d_2 + \Lambda_2 \xi_2). \end{aligned} \tag{23}$$

To force the time derivative of V_2 to be negative definite, the virtual control v_2 and the dynamics of ε_1 are chosen as

$$v_2 = g_2^{-1}(\Lambda_2 \xi_2 + \dot{v}_{1,f} - f_2 + g_1^\top \overline{z}_1 - \hat{d}_2 + A_2 z_2), \tag{24}$$

$$\dot{\varepsilon}_1 = -A_1 \varepsilon_1 - \Lambda_1 \chi_1 + g_1(v_1 - v_{1,f} + \varepsilon_2), \quad \varepsilon_1(0) = 0, \tag{25}$$

where $\hat{d}_2$ is the disturbance estimate signal generated by a disturbance observer, while $A_2 = A_2^\top \in \mathbb{R}^{n_2 \times n_2}$ is a diagonal positive definite matrix. With Assumption 2, the matrix g_2 is guaranteed to be non-singular for all x_1,x_2. Thus using Eqs. (24) and (25), and neglecting the disturbance estimation errors, it can be easily verified that Eq. (23) can be written as

$$\dot{V}_2 = -\overline{z}_1^\top A_1 \overline{z}_1 - z_2^\top A_2 z_2 + \overline{z}_1^\top g_1 \varepsilon_2, \tag{26}$$

where $\overline{z}_1$ is given by Eq. (20). At this point in the design process, the negative definiteness of $\dot{V}_2$ is not guaranteed due to the last term in Eq. (26). However, this term will be canceled out during the next step of the controller design. Before moving on to the next stage, the disturbance estimate $\hat{d}_2$ in Eq. (24) is generated using the same nonlinear disturbance observer (7) with its equations depicted by

$$\dot{\delta}_2 = -\mu_2 \delta_2 - \mu_2^2 x_2 - \mu_2(f_2 + g_2 v_2), \quad \delta_2(0) = -\mu_2 x_{20}, \tag{27}$$

$$\hat{d}_2 = \delta_2 + \mu_2 x_2, \tag{28}$$

Please cite this article as: R. Rashad, et al., A novel disturbance observer-based backstepping controller with command filtered compensation for a MIMO system, Journal of the Franklin Institute. (2016), http://dx.doi.org/10.1016/j.jfranklin.2016.07.017

where $\mu_2 > 0$ represents the observer gain. Similar to the disturbance observer designed in the previous subsection, the disturbance estimation error e_{d_2} and its associated dynamics are given by

$$e_{d_2} = \hat{d}_2 - d_2 \tag{29}$$

$$\dot{e}_{d_2} = -\mu_2 e_{d_2} - \dot{d}_2, \quad e_{d_2}(0) = -d_{20}, \tag{30}$$

where $d_{20} = d_2(0)$. This concludes the second stage of the controller design. The stability analysis of the overall closed loop system will be presented in a subsequent section of the article.

3.3. Controller design step 3

The final step in the controller design considers the last subsystem given by

$$\dot{x}_3 = f_3 + g_3 u + d_3. \tag{31}$$

The backstepping variables are selected as

$$z_3 = v_{2,f} - x_3, \quad \xi_3 = \int_0^t z_3(\tau)d\tau, \quad \xi_3(0) = 0, \tag{32}$$

where $v_{2,f} \in \mathbb{R}^{n_3}$ represents the filtered command signal generated using the first order low pass filter

$$\dot{v}_{2,f} = \gamma(v_2 - v_{2,f}), \quad v_{2,f}(0) = v_{20}, \tag{33}$$

where γ is the filter's cut-off frequency, whereas $v_{20} = v_2(x_{10}, x_{20}, v_{10})$ denotes the initial value of the virtual control signal (24). Similar to the derivation of $\dot{z}_1$ detailed in Eqs. (16)–(19), the derivative of z_2 can be written using Eqs. (24), (29), and (32) as

$$\dot{z}_2 = -A_2 z_2 - \Lambda_2 \xi_2 + e_{d_2} - g_1^\top \bar{z}_1 + g_2 z_3 + g_2(v_2 - v_{2,f}). \tag{34}$$

We then proceed by compensating for the second command filter (33) using the new vector $\varepsilon_2 \in \mathbb{R}^{n_2}$ and define

$$\bar{z}_2 = z_2 - \varepsilon_2, \quad \bar{\xi}_2 = \int_0^t \bar{z}_2(\tau)d\tau = \xi_2 - \chi_2, \tag{35}$$

where $\chi_2 = \int_0^t \varepsilon_2(\tau)d\tau$. Then we introduce the augmented Lyapunov function

$$V_3 = \tfrac{1}{2}\bar{z}_1^\top \bar{z}_1 + \tfrac{1}{2}\bar{\xi}_1^\top \Lambda_1 \bar{\xi}_1 + \tfrac{1}{2}\bar{z}_2^\top \bar{z}_2 + \tfrac{1}{2}\bar{\xi}_2^\top \Lambda_2 \bar{\xi}_2 + \tfrac{1}{2} z_3^\top z_3 + \tfrac{1}{2}\xi_3^\top \Lambda_3 \xi_3, \tag{36}$$

where $\Lambda_3 = \Lambda_3^\top \in \mathbb{R}^{n_3 \times n_3}$ is a diagonal positive definite matrix. Similar to the derivation of $\dot{V}_2$ detailed in Eqs. (22)–(23), and by using Eqs. (19), (31), (34) in addition to neglecting all disturbance estimation errors, the time derivative of V_3 can be written as

$$\begin{aligned}\dot{V}_3 = &-\bar{z}_1^\top A_1 \bar{z}_1 + \bar{z}_2^\top(-A_2 z_2 - \Lambda_2 \chi_2 + g_2(v_2 - v_{2,f}) - \dot{\varepsilon}_2) \\ &+ z_3^\top(g_2^\top \bar{z}_2 + \dot{v}_{2,f} - f_3 - g_3 u - d_3 + \Lambda_3 \xi_3).\end{aligned} \tag{37}$$

In order for the time derivative of V_3 to be negative definite, the actual control signal u and the dynamics of ε_2 are chosen as

$$u = g_3^{-1}(\Lambda_3 \xi_3 + \dot{v}_{2,f} - f_3 + g_2^\top \bar{z}_2 - \hat{d}_3 + A_3 z_3), \tag{38}$$

$$\dot{\varepsilon}_2 = -A_2 \varepsilon_2 - \Lambda_2 \chi_2 + g_2(v_2 - v_{2,f}), \quad \varepsilon_2(0) = 0, \tag{39}$$

where $A_3 = A_3^\top \in \mathbb{R}^{n_3 \times n_3}$ is a diagonal positive definite matrix. The existence of the inverse

Please cite this article as: R. Rashad, et al., A novel disturbance observer-based backstepping controller with command filtered compensation for a MIMO system, Journal of the Franklin Institute. (2016), http://dx.doi.org/10.1016/j.jfranklin.2016.07.017

matrix g_3^{-1} is guaranteed by Assumption 2. Thus using Eqs. (38) and (39), the function $\dot{V}_3$ is simplified to

$$\dot{V}_3 = -\bar{z}_1^\top A_1 \bar{z}_1 - \bar{z}_2^\top A_2 \bar{z}_2 - z_3^\top A_3 z_3 < 0, \quad \forall \bar{z}_1, \bar{z}_2, z_3 \neq 0. \tag{40}$$

The disturbance observer generating an estimate for d_3 is depicted by

$$\dot{\delta}_3 = -\mu_3 \delta_3 - \mu_3^2 x_3 - \mu_3 (f_3 + g_3 u), \quad \delta_3(0) = -\mu_3 x_{30}, \tag{41}$$

$$\hat{d}_3 = \delta_3 + \mu_3 x_3, \tag{42}$$

where $\mu_3 > 0$ represents the observer gain. Finally, the disturbance estimation error e_{d_3} and its associated dynamics are given by

$$e_{d_3} = \hat{d}_3 - d_3 \tag{43}$$

$$\dot{e}_{d_3} = -\mu_3 e_{d_3} - \dot{d}_3, \quad e_{d_3}(0) = -d_{30}, \tag{44}$$

where $d_{30} = d_3(0)$. Before moving to the next section, the time derivative of the last backstepping variable z_3 is presented as it will be required in subsequent sections. It is given by

$$\dot{z}_3 = -A_3 z_3 - \Lambda_3 \xi_3 + e_{d_3} - g_2^\top \bar{z}_2, \tag{45}$$

and its derivation is similar to the derivation of Eqs. (19) and (34).

3.4. Controller gains design considerations

The presented control approach contains several gains which act as tuning parameters to be chosen by the designer. For each stage $i = \{1, 2, 3\}$, the choice of matrices A_i, Λ_i in addition to the gains μ_i and γ affects the stability and performance of the overall closed loop system.

To maintain the stability of the closed loop system, the gain matrices A_i, Λ_i are designed such that each matrix

$$J_i \triangleq \begin{bmatrix} 0 & I_i \\ -\Lambda_i & -A_i \end{bmatrix}, \quad i = 1, 2, 3,$$

is Hurwitz, where I_i denotes the identity matrix of size n_i. The justification of this criteria will be clear in the coming section when the stability analysis is presented.

To guarantee a satisfactory tracking performance, it is standard in vectorial backstepping to choose $\lambda_{min}(J_1) > \lambda_{min}(J_2) > \lambda_{min}(J_3)$, where $\lambda_{min}(J_i)$ denotes the minimum eigenvalue of the matrix J_i. This guarantees that the backstepping variables converge in a sequential manner, i.e., z_3 converges faster than z_2, which converges faster than z_1. Moreover, the disturbance observer gains μ_i should be assigned large values to ensure a fast convergence of the disturbance estimation error as implied by Eqs. (10), (30), and (44). However as a consequence, this can cause high transients in the control signal which can degrade the tracking performance of the overall system as implied by Eqs. (8), (28), and (42). Moreover, assigning the low pass filter's cut-off frequency γ a large value ensures that the signals $\upsilon_{i,f}$ will accurately track υ_i. However, this will introduce high frequency noise in the control signals as a consequence. This in turn will degrade the tracking performance in practical applications due to the excitation of the high frequency unmodeled dynamics available in the system. Thus, the designer has to compromise between these aspects to yield the most satisfactory performance.

Please cite this article as: R. Rashad, et al., A novel disturbance observer-based backstepping controller with command filtered compensation for a MIMO system, Journal of the Franklin Institute. (2016), http://dx.doi.org/10.1016/j.jfranklin.2016.07.017

4. Closed loop system analysis

The stability proof of the overall closed loop system based on singular perturbation theory, similar to [8], will be presented in this section. The stability analysis will use Tikhonov's theorem (Theorem 11.2 in [1]) which is too long to allow its inclusion in this article. Therefore, to simplify the interpretation of the results of this section in terms of that theorem, this section's terminology and all technical statements presented correspond to the requirements of Theorem 11.2. In Section 4.1, the standard singular perturbation model will be formulated and it will be shown that all preconditions of Tikhonov's theorem are satisfied. In Section 4.2, a summary of the stability properties of the proposed control approach will be presented.

4.1. Stability proof

Let $y(t,\epsilon)$ be a time signal, where ϵ is a positive gain parameter that influences the generation of the signal. Throughout this section we will use the notation $y(t,\epsilon)=\mathcal{O}(\epsilon)$ which is defined as follows [1].

Definition 1. The signal $y(t,\epsilon)$ is said to be of order ϵ, denoted as $y(t,\epsilon)=\mathcal{O}(\epsilon)$, if there exists positive constants k and c such that $|y(t,\epsilon)|\le k|\epsilon|$, $\forall\,|\epsilon|<c$ and $t\ge 0$.

Remark 1. The perturbation parameter ϵ used in this article will be chosen as $\epsilon=1/\gamma$, i.e., the reciprocal of the command filter's cut-off frequency. Moreover, we assume that observer gains μ_i are designed to be the same order of magnitude as γ, i.e., $\mathcal{O}(\mu_i)=\mathcal{O}(\gamma)$. Thus, we can write the observer gains as multiples of ϵ [20]. Therefore for $i=\{1,2,3\}$, we write $1/\mu_i=\alpha_i\epsilon$, where $\alpha_i=\gamma/\mu_i$ are positive known constants.

First we define the vectors $\hat{x}\in\mathbb{R}^{4n-2n_3}$ and $\hat{z}\in\mathbb{R}^{2n-n_1}$

$$\hat{x}=\left[\xi_1^\top,z_1^\top,\xi_2^\top,z_2^\top,\xi_3^\top,z_3^\top,\chi_1^\top,\varepsilon_1^\top,\chi_2^\top,\varepsilon_2^\top\right]^\top \tag{46}$$

$$\hat{z}=\left[\hat{z}_1^\top,\hat{z}_2^\top,\hat{z}_3^\top,\hat{z}_4^\top,\hat{z}_5^\top\right]^\top=\left[v_{1f}^\top,v_{2f}^\top,e_{d_1}^\top,e_{d_2}^\top,e_{d_3}^\top\right]^\top. \tag{47}$$

The standard singular perturbation model is given by

$$\dot{\hat{x}}=\hat{f}(t,\hat{x},\hat{z},\epsilon) \tag{48}$$

$$\epsilon\dot{\hat{z}}=\hat{g}(t,\hat{x},\hat{z},\epsilon), \tag{49}$$

where $\hat{f}$ and $\hat{g}$ are defined below. The initial conditions, defined in Section 3 are given by

$$\begin{aligned}\hat{x}(0)&=\left[0_{n_1},x_{d0}^\top-x_{10}^\top,0_{n_2},v_{10}^\top-x_{20}^\top,0_{n_3},v_{20}^\top-x_{30}^\top,0_{n_1},0_{n_1},0_{n_2},0_{n_2}\right]^\top\\ \hat{z}(0)&=\left[v_{10}^\top,v_{20}^\top,-d_{10}^\top,-d_{20}^\top,-d_{30}^\top\right]^\top,\end{aligned} \tag{50}$$

where 0_{n_i} is a zero row vector with dimensions n_i. It is worth noting that these initial conditions are independent of ϵ.

The vector field $\hat{f}$, as derived based on Eqs. (19), (25), (34), (39), (45) is given by

$$\hat{f}_1(t,\hat{x},\hat{z},\epsilon)=z_1$$

Please cite this article as: R. Rashad, et al., A novel disturbance observer-based backstepping controller with command filtered compensation for a MIMO system, Journal of the Franklin Institute. (2016), http://dx.doi.org/10.1016/j.jfranklin.2016.07.017

$$\begin{aligned}
\hat{f}_2(t,\hat{x},\hat{z},\epsilon) &= -A_1 z_1 - \Lambda_1 \xi_1 + g_1 z_2 + g_1 v_1 - g_1 \hat{z}_1 + \hat{z}_3 \\
\hat{f}_3(t,\hat{x},\hat{z},\epsilon) &= z_2 \\
\hat{f}_4(t,\hat{x},\hat{z},\epsilon) &= -A_2 z_2 - \Lambda_2 \xi_2 - g_1^{\top}(z_1 - \varepsilon_1) + g_2 z_3 + g_2 v_2 - g_2 \hat{z}_2 + \hat{z}_4 \\
\hat{f}_5(t,\hat{x},\hat{z},\epsilon) &= z_3 \\
\hat{f}_6(t,\hat{x},\hat{z},\epsilon) &= -A_3 z_3 - \Lambda_3 \xi_3 - g_2^{\top}(z_2 - \varepsilon_2) + \hat{z}_5 \\
\hat{f}_7(t,\hat{x},\hat{z},\epsilon) &= \varepsilon_1 \\
\hat{f}_8(t,\hat{x},\hat{z},\epsilon) &= -A_1 \varepsilon_1 - \Lambda_1 \chi_1 + g_1 \varepsilon_2 + g_1 v_1 - g_1 \hat{z}_1 \\
\hat{f}_9(t,\hat{x},\hat{z},\epsilon) &= \varepsilon_2 \\
\hat{f}_{10}(t,\hat{x},\hat{z},\epsilon) &= -A_2 \varepsilon_2 - \Lambda_2 \chi_2 + g_2 v_2 - g_2 \hat{z}_2,
\end{aligned} \tag{51}$$

where $\hat{z}_i$ are given by Eq. (47), noting that $\dot{\xi}_i = z_i$ and $\dot{\chi}_i = \varepsilon_i$. Note that the function $\hat{f}$ is independent of ϵ and with Assumptions 1–4, $\hat{f}$ and its first partial derivatives with respect to $(\hat{x},\hat{z},\epsilon)$ are continuous and bounded on any compact set $\mathcal{D}_{\hat{x}} \times \mathcal{D}_{\hat{z}}$. The two sets $\mathcal{D}_{\hat{x}} \subset \mathbb{R}^{4n-2n_3}$ and $\mathcal{D}_{\hat{z}} \subset \mathbb{R}^{2n-n_1}$ are compact sets that contain the origin.

The vector field $\hat{g}$, as derived based on Eqs. (10), (15), (30), (33), (44), is given by

$$\begin{aligned}
\hat{g}_1(t,\hat{x},\hat{z},\epsilon) &= v_1 - \hat{z}_1 \\
\hat{g}_2(t,\hat{x},\hat{z},\epsilon) &= v_2 - \hat{z}_2 \\
\hat{g}_3(t,\hat{x},\hat{z},\epsilon) &= -(1/\alpha_1)\hat{z}_3 - \epsilon \dot{d}_1 \\
\hat{g}_4(t,\hat{x},\hat{z},\epsilon) &= -(1/\alpha_2)\hat{z}_4 - \epsilon \dot{d}_2 \\
\hat{g}_5(t,\hat{x},\hat{z},\epsilon) &= -(1/\alpha_3)\hat{z}_5 - \epsilon \dot{d}_3,
\end{aligned} \tag{52}$$

where α_i are defined in Remark 1. Note that with Assumptions 1–4, on any compact set $\mathcal{D}_{\hat{x}} \times \mathcal{D}_{\hat{z}}$: the function $\hat{g}$ and its first partial derivatives with respect to $(\hat{x},\hat{z},\epsilon)$ are continuous and bounded, and $(\partial \hat{g}/\partial t)$ is continuous and bounded in addition that $\partial \hat{g}(t,\hat{x},\hat{z},0)/\partial \hat{z}$ has bounded first partial derivatives with respect to its arguments.

Remark 2. As observed in Eqs. (11), (24), the virtual control signals are computed using the disturbance estimates $\hat{d}_i$. In the singular perturbation model (48) and (49) these estimates are replaced by $e_{d_i} + d_i$ (cf. Eqs. (9) and (29)) where $e_{d_1} = \hat{z}_3$ and $e_{d_2} = \hat{z}_4$. Thus, the virtual control signals are independent of ϵ.

For $\epsilon = 0$, the unique solution to Eq. (49) will be denoted by $\hat{z} = \hat{h}(t,\hat{x})$ and is given by

$$\hat{z} = \hat{h}(t,\hat{x}) = \left[v_1^{\top}, v_2^{\top}, 0_{n_1}, 0_{n_2}, 0_{n_3}\right]^{\top}. \tag{53}$$

With Assumptions 1–3, on any compact set $\mathcal{D}_{\hat{x}}$, the function $\hat{h}(t,\hat{x})$ has bounded first partial derivatives with respect to its arguments.

Now we define $\tilde{x}(t)$ to be the solution of the reduced model which is obtained by substituting Eq. (53) in Eq. (48) at $\epsilon = 0$ [1, Eq. (11.5), p. 424]. The reduced model's state equations are given by

$$\dot{\tilde{x}} = \hat{f}(t,\tilde{x},\hat{h}(t,\tilde{x}),0), \quad \tilde{x}(0) = \hat{x}(0). \tag{54}$$

Note that with Assumption 1, the function $\partial \hat{f}(t,\tilde{x},\hat{h}(t,\tilde{x}),0)/\partial \tilde{x}$ is Lipschitz $\tilde{x}$, uniformly in t (cf. Eq. (57)). In the reduced order model (54), by inspecting $\hat{f}_9$ and $\hat{f}_{10}$ which are depicted by

$$\hat{f}_9(t,\tilde{x},\hat{h}(t,\tilde{x}),0) = \varepsilon_2 \tag{55}$$

$$\hat{f}_{10}(t,\tilde{x},\hat{h}(t,\tilde{x}),0) = -A_2 \varepsilon_2 - \Lambda_2 \chi_2, \tag{56}$$

Please cite this article as: R. Rashad, et al., A novel disturbance observer-based backstepping controller with command filtered compensation for a MIMO system, Journal of the Franklin Institute. (2016), http://dx.doi.org/10.1016/j.jfranklin.2016.07.017

and the fact that the initial conditions for ε_2 and χ_2 are zeros (cf. Eq. (50)), it can be deduced that these signals will remain zero for all $t>0$. Furthermore, the same argument holds for the signals ε_1 and χ_1. Therefore, excluding the states ε_i and χ_i from the state vector $\tilde{x}$, we can rewrite the reduced model as

$$\dot{\tilde{x}} = \begin{bmatrix} \dot{\tilde{\xi}}_1 \\ \dot{\tilde{z}}_1 \\ \dot{\tilde{\xi}}_2 \\ \dot{\tilde{z}}_2 \\ \dot{\tilde{\xi}}_3 \\ \dot{\tilde{z}}_3 \end{bmatrix} = \begin{bmatrix} \tilde{z}_1 \\ -A_1\tilde{z}_1 - \Lambda_1\tilde{\xi}_1 + g_1\tilde{z}_2 \\ \tilde{z}_2 \\ -A_2\tilde{z}_2 - \Lambda_2\tilde{\xi}_2 - g_1^\top\tilde{z}_1 + g_2\tilde{z}_3 \\ \tilde{z}_3 \\ -A_3\tilde{z}_3 - \Lambda_3\tilde{\xi}_3 - g_2^\top\tilde{z}_2 \end{bmatrix}, \tag{57}$$

which can be written in compact form as

$$\dot{\tilde{x}} = -\Gamma\tilde{x} + \Gamma_{ss}(t,\tilde{x})\tilde{x}, \tag{58}$$

where $\Gamma \in \mathbb{R}^{2n\times 2n}$ is a constant block diagonal matrix with 3 blocks each defined by

$$J_i = \begin{bmatrix} 0 & -I_i \\ \Lambda_i & A_i \end{bmatrix} \in \mathbb{R}^{2n_i\times 2n_i} \tag{59}$$

whereas $\Gamma_{ss} \in \mathbb{R}^{2n\times 2n}$ is a time varying skew-symmetric matrix given by

$$\Gamma_{ss}(t,\tilde{x}) = \begin{bmatrix} \mathbf{0} & \mathbf{0} & \mathbf{0} & \mathbf{0} & \mathbf{0} & \mathbf{0} \\ \mathbf{0} & \mathbf{0} & \mathbf{0} & g_1(t,\tilde{x}) & \mathbf{0} & \mathbf{0} \\ \mathbf{0} & \mathbf{0} & \mathbf{0} & \mathbf{0} & \mathbf{0} & \mathbf{0} \\ \mathbf{0} & -g_1^\top(t,\tilde{x}) & \mathbf{0} & \mathbf{0} & \mathbf{0} & g_2(t,\tilde{x}) \\ \mathbf{0} & \mathbf{0} & \mathbf{0} & \mathbf{0} & \mathbf{0} & \mathbf{0} \\ \mathbf{0} & \mathbf{0} & \mathbf{0} & -g_2^\top(t,\tilde{x}) & \mathbf{0} & \mathbf{0} \end{bmatrix}, \tag{60}$$

where $\mathbf{0}$ is a matrix of zeros of appropriate dimensions. A requirement of Tikhonov's theorem is that the origin must be an exponentially stable equilibrium of the reduced order system (54). Due to the aforementioned fact about ε_i and χ_i in the reduced model, it is sufficient to only consider the origin of the non-autonomous system (58). Consider the following Lyapunov function

$$\tilde{V} = \tfrac{1}{2}\tilde{x}^\top\tilde{x} = \tfrac{1}{2}\|\tilde{x}\|_2^2. \tag{61}$$

The time derivative of $\tilde{V}$ along the solutions of Eq. (58) is given by

$$\dot{\tilde{V}} = \tilde{x}^\top\dot{\tilde{x}} = \tilde{x}^\top(-\Gamma + \Gamma_{ss})\tilde{x} = -\tilde{x}^\top\Gamma\tilde{x} + \tilde{x}^\top\Gamma_{ss}\tilde{x}. \tag{62}$$

Using the fact that the matrix Γ_{ss} satisfies $\tilde{x}^\top\Gamma_{ss}\tilde{x} = 0, \forall\tilde{x}$, we can rewrite Eq. (62) as

$$\dot{\tilde{V}} = -\tilde{x}^\top\Gamma\tilde{x} \le -\lambda_{min}(\Gamma)\|\tilde{x}\|_2^2 = -2\lambda_{min}(\Gamma)\tilde{V}, \tag{63}$$

where $\lambda_{min}(\Gamma)$ is the minimum eigenvalue of Γ. By designing the controller gains Λ_i, A_i such that each matrix (59) is positive definite, we will guarantee that $\lambda_{min}(\Gamma)>0$. Therefore, by Theorem 4.10 in [1], the equilibrium $\tilde{x}=0$ of system (58) is globally exponentially stable. Moreover, due to the fact that ε_i and χ_i are zero for all $t>0$, the origin of the reduced model (54) is also globally exponentially stable.

Please cite this article as: R. Rashad, et al., A novel disturbance observer-based backstepping controller with command filtered compensation for a MIMO system, Journal of the Franklin Institute. (2016), http://dx.doi.org/10.1016/j.jfranklin.2016.07.017

Now we define $\hat{y} \triangleq \hat{z} - \hat{h}(t,\hat{x})$, and the boundary layer model [1, eqn. (11.14), p. 433] is defined by

$$\frac{d\hat{y}}{d\tau} = \hat{g}\left(t, \hat{x}, \hat{y} + \hat{h}(t,\hat{x}), 0\right), \tag{64}$$

with $(t,\hat{x})$ considered fixed and $\tau = t/\epsilon$. The vector $\hat{y} \in \mathbb{R}^{2n-n_1}$ consists of $\hat{y} = \left[\hat{y}_1^\top, \hat{y}_2^\top, \hat{y}_3^\top, \hat{y}_4^\top, \hat{y}_5^\top\right]^\top$ similar to Eq. (47). Using Eqs. (52) and (53), we can rewrite the boundary layer model (64) as

$$\frac{d\hat{y}}{d\tau} = \begin{bmatrix} -\hat{y}_1 \\ -\hat{y}_2 \\ -(1/\alpha_1)\hat{y}_3 \\ -(1/\alpha_2)\hat{y}_4 \\ -(1/\alpha_3)\hat{y}_5 \end{bmatrix} = \Gamma_B \hat{y}, \tag{65}$$

where Γ_B is a diagonal Hurwitz matrix with entries of (-1) and $(-1/\alpha_i)$ only, with $\alpha_i > 0$ defined in Remark 1. Therefore, the origin $\hat{y} = 0$ is a globally exponentially stable equilibrium of the boundary layer model (64). It is also worth noting that the boundary layer model is linear and independent of $\hat{x}$.

At this point, all conditions of Theorem 11.2 in [1] hold on any compact set $\mathcal{D}_{\hat{x}} \times \mathcal{D}_{\hat{z}}$. Then, if we denote the solutions to Eqs. (48), (49) and (54) respectively, as $\hat{x}(t,\epsilon)$, $\hat{z}(t,\epsilon)$ and $\tilde{x}(t,\epsilon)$, we have for all $t > 0$ the following properties:

$$\hat{x}(t,\epsilon) - \tilde{x}(t,\epsilon) = \mathcal{O}(\epsilon)$$
$$\hat{z}(t,\epsilon) - \hat{h}(t,\hat{x}) - \overline{y}(t/\epsilon) = \mathcal{O}(\epsilon),$$

where $\overline{y}(t/\epsilon)$ is the solution of the autonomous system [1, eqn. (11.13), p. 432] given by

$$\frac{d\overline{y}}{d\tau} = \hat{g}\left(0, \hat{x}(0), \overline{y} + \hat{h}(0,\hat{x}(0)), 0\right), \tag{66}$$

with initial conditions

$$\overline{y}(0) = \hat{z}(0) - \hat{h}(0,\hat{x}(0)) = \left[0_{n_2}, 0_{n_3}, -d_{10}^\top, -d_{20}^\top, -d_{30}^\top\right]^\top. \tag{67}$$

This concludes the stability properties of the overall closed loop system.

4.2. Summary of stability properties

The stability properties of the DOB control scheme presented in this article will be summarized in this section. For the system described by Eq. (1) that satisfies Assumptions 1–4 with the controller defined by Eq. (38), we have the following properties for all $t > 0$:

(1) $z_i(t,\epsilon) - \tilde{z}_i(t,\epsilon) = \mathcal{O}(\epsilon)$;
(2) $\xi_i(t,\epsilon) - \tilde{\xi}_i(t,\epsilon) = \mathcal{O}(\epsilon)$;
(3) $e_{d_i}(t,\epsilon) - \overline{y}_{i+2}(t/\epsilon) = \mathcal{O}(\epsilon)$, for $i = \{1,2,3\}$; and,
(4) $v_{i,f}(t,\epsilon) - v_i(t,\epsilon) = \mathcal{O}(\epsilon)$, for $i = \{1,2\}$.

The signals v_i are defined in Eqs. (11) and (24), $\tilde{z}_i$ and $\tilde{\xi}_i$ are the solutions to Eq. (57), and $z_i(t,\epsilon)$ denote the backstepping variables (3), (14), (32) for a specific choice of the command filter's cut-off frequency γ and the disturbance observer gains μ_i. Specifically, the signal $z_1(t,\epsilon)$ represents

Please cite this article as: R. Rashad, et al., A novel disturbance observer-based backstepping controller with command filtered compensation for a MIMO system, Journal of the Franklin Institute. (2016), http://dx.doi.org/10.1016/j.jfranklin.2016.07.017

the tracking error, which will be bounded for all $t>0$. Moreover, for $i=\{1,2,3\}$, the signals $\overline{y}_{i+2}(t/\epsilon)$ denote the elements of $\overline{y}(t/\epsilon)$ defined in Section 4.1.

Based on the stability proof presented, by increasing the gains γ and μ_i, the tracking error bound can be reduced. Moreover, the solution to the disturbance observer-based closed loop system can be made arbitrarily close to the system (57) which was proved to be globally exponentially stable. However, in practice increasing these gains have other consequences discussed in Section 3.4. Thus, a compromise has to be performed by the designer to yield the most satisfactory performance.

5. Case study: twin rotor MIMO system

The TRMS is a laboratory setup designed for flight control experiments as shown in Fig. 1. It is perceived as a static test rig for a helicopter with several control challenges [21]. It consists of two rotors, the tail rotor and main rotor, driven by DC motors perpendicular to each other. The two rotors are connected by a beam pivoted on its base such that it can rotate in both the horizontal and vertical planes. The motion of the beam is damped by a counterbalance arm with a weight at its end hanging from the central pivot point. The input to the TRMS is the supply voltages of the DC motors which consequently change the aerodynamic forces generated by the propellers through the speeds of the two rotors. The TRMS is equipped with angular position sensors that measure the vertical and horizontal angles known as the pitch and yaw, respectively. Moreover, the angular velocity of each rotor is measured using tachogenerators coupled with each DC motor.

5.1. Mathematical model

The mathematical model of the TRMS has been developed in several studies [22,23] using Newton's second law of motion. Throughout this article, the subscripts (h) and (v) will denote the horizontal and vertical axes respectively. A state space formulation of the TRMS model can be found in [10,16]. The state space equations are developed for the state vector and input vector given by

$$\begin{aligned} x_p &= [x_{11}, x_{12}, x_{21}, x_{22}, x_{31}, x_{32}]^\top = [\alpha_h, \alpha_v, \Omega_h, \Omega_v, u_{hh}, u_{vv}]^\top, \\ u_p &= [U_h, U_v]^\top, \end{aligned} \tag{68}$$

and a summary of the state space model is given below

$$\begin{aligned} \dot{x}_{11} &= x_{21} \\ \dot{x}_{12} &= x_{22} \\ \dot{x}_{21} &= \frac{1}{J_h}\Big[F_h l_t \cos x_{12} - f_h x_{21} - J_{mr}\omega_v x_{22}\sin x_{12} \\ &\quad - x_{21}x_{22}(D-E)\sin(2x_{12}) + \frac{J_{mr}}{T_{mr}}(U_v - x_{32})\frac{dP_{v1}}{dx_{32}}\cos x_{12}\Big] \\ \dot{x}_{22} &= \frac{1}{J_v}\Big[F_v l_m - f_v x_{22} + g[(A-B)\cos x_{12} - C\sin x_{12}] \\ &\quad - x_{21}^2(A+B+C)\cos x_{12}\sin x_{12} + \frac{J_{tr}}{T_{tr}}(U_h - x_{31})\frac{dP_{h1}}{dx_{31}}\Big] \end{aligned}$$

Please cite this article as: R. Rashad, et al., A novel disturbance observer-based backstepping controller with command filtered compensation for a MIMO system, Journal of the Franklin Institute. (2016), http://dx.doi.org/10.1016/j.jfranklin.2016.07.017

$$\dot{x}_{31} = \frac{1}{T_{tr}}(U_h - x_{31})$$
$$\dot{x}_{32} = \frac{1}{T_{mr}}(U_v - x_{32}). \tag{69}$$

The parameters in Eq. (69) are defined as follows: α_h, α_v are the yaw and pitch angles of TRMS beam, Ω_h, Ω_v are the yaw and pitch angular rates of the beam, F_h,F_v are the propeller thrust forces generated, l_t,l_m are the lengths of the tail part and main part of the beam, f_h,f_v are the viscous friction coefficients, T_{mr}, T_{tr} are the main rotor and tail rotor time constants, U_h,U_v are the supply voltages while u_{hh}, u_{vv} are their filtered counterparts, J_{tr}, J_{mr} are constant moments of inertia of the tail and main propellers in their axes, J_h,J_v are moments of inertia functions in the horizontal and vertical axes, and g denotes the gravitational acceleration. The moment of inertia function J_h is given as $J_h(\alpha_v) = D\sin^2(\alpha_v) + E\cos^2(\alpha_v) + F$. Finally, the terms A, B, C, D, E, F are constants depending on the geometrical and mass properties of the TRMS defined as

$$A = \left(\frac{m_t}{2} + m_{tr} + m_{ts}\right) l_t, \quad B = \left(\frac{m_m}{2} + m_{mr} + m_{ms}\right) l_m,$$
$$C = \frac{m_b}{2} l_b + m_{cb} l_{cb}, \quad D = \frac{m_b}{3} l_b^2 + m_{cb} l_{cb}^2,$$
$$E = \left(\frac{m_t}{3} + m_{tr} + m_{ts}\right) l_t^2 + \left(\frac{m_m}{3} + m_{mr} + m_{ms}\right) l_m^2,$$
$$F = m_{ms} r_{ms}^2 + \frac{m_{ts}}{2} r_{ts}^2,$$

where $m_{mr}(m_{tr})$ is the mass of the main(tail) DC motor with main(tail) rotor, $m_m(m_t)$ is the mass of the main(tail) part of the beam, $m_{ms}(m_{ts})$ is the mass of the main(tail) shield surrounding the propellers, $r_{ms}(r_{ts})$ is the radius of the main(tail) shield, m_b, m_{cb} are the masses of the counterweight and the counterweight beam and l_b, l_{cb} are the length of the counterweight beam and the distance between the counterweight and the joint.

In the TRMS model, the rotors are modeled as linear systems followed by a static nonlinearity [14]. Their linear models are first order systems given by the last two equations in Eq. (69). The two static nonlinear smooth functions which determine the dependance of the DC motor angular velocity on input voltage are given by

$$\omega_h = P_{h1}(u_{hh}), \quad \omega_v = P_{v1}(u_{vv}), \tag{70}$$

while the dependance of the propeller thrust on the motor angular velocity is characterized by two nonlinear smooth functions given by

$$F_h = P_{h2}(\omega_h), \quad F_v = P_{v2}(\omega_v), \tag{71}$$

which are identified experimentally using an electronic balance instead of performing aerodynamic modeling of the rotors [23].

5.2. Problem formulation

The control problem considered in this paper is the asymptotic tracking of a reference trajectory x_1^d for the yaw and pitch angles of the TRMS. This desired trajectory is assumed to satisfy Assumption 3. For the controller design, the state space equations of the TRMS (69) will be rewritten as three subsystems as follows

$$\dot{x}_1 = x_2$$
$$\dot{x}_2 = f_1(x_1, x_2) + g_1(x_1)\rho_1(x_3) + d_1$$

Please cite this article as: R. Rashad, et al., A novel disturbance observer-based backstepping controller with command filtered compensation for a MIMO system, Journal of the Franklin Institute. (2016), http://dx.doi.org/10.1016/j.jfranklin.2016.07.017

$$\dot{x}_3 = f_2(x_3) + g_2 u_p$$
$$y = x_1, \tag{72}$$

where $x_1 = [x_{11}, x_{12}]^\top, x_2 = [x_{21}, x_{22}]^\top, x_3 = [x_{31}, x_{32}]^\top$, and the vectors f_1 and f_2 are given by

$$f_1(x_1, x_2) = [f_{1_h}, f_{1_v}]^\top$$
$$f_{1_h}(x_1, x_2) = \frac{1}{J_h}\left[-f_h x_{21} - J_{mr}\omega_v x_{22}\sin x_{12} - x_{21}x_{22}(D-E)\sin(2x_{12})\right]$$
$$f_{1_v}(x_1, x_2) = \frac{1}{J_v}\left[-f_v x_{22} + g((A-B)\cos x_{12} - C\sin x_{12}) - x_{12}^2(A+B+C)\cos x_{12}\sin x_{12}\right]$$

$$f_2(x_3) = \left[-\frac{x_{31}}{T_{tr}}, -\frac{x_{32}}{T_{mr}}\right]^\top, \tag{73}$$

while the matrices g_1, g_2 are given by

$$g_1(x_1) = \begin{bmatrix} \dfrac{l_t \cos x_{12}}{J_h(x_{12})} & 0 \\ 0 & \dfrac{l_m}{J_v} \end{bmatrix}, \quad g_2 = \begin{bmatrix} \dfrac{1}{T_{tr}} & 0 \\ 0 & \dfrac{1}{T_{mr}} \end{bmatrix}. \tag{74}$$

Moreover, using Eqs. (70)–(71), the vector ρ_1 can be written as

$$\rho_1(x_3) = \begin{bmatrix} F_h \\ F_v \end{bmatrix} = \begin{bmatrix} P_{h2}(\omega_h) \\ P_{v2}(\omega_v) \end{bmatrix} = \begin{bmatrix} P_{h2}(P_{h1}(x_{31})) \\ P_{v2}(P_{v1}(x_{32})) \end{bmatrix}, \tag{75}$$

which is a continuously differentiable function of x_3. Finally the disturbance vector d_1 consists of

$$d_1 = \begin{bmatrix} \frac{1}{J_h}\left[\frac{J_{mr}}{T_{mr}}(U_v - x_{32})\frac{dP_{v1}}{dx_{32}}\cos x_{12}\right] + d_{h,ext} \\ \frac{1}{J_v}\left[\frac{J_{tr}}{T_{tr}}(U_h - x_{31})\frac{dP_{h1}}{dx_{31}}\right] + d_{v,ext} \end{bmatrix}, \tag{76}$$

where $d_{h,ext}, d_{v,ext}$ represent unmodeled external disturbances which may occur due to partial actuator failure.

By this formulation it can be observed that the state equations are in a quasi-strict feedback structure. Thus a suitable control approach would be to use the backstepping technique by considering x_2 as a virtual input to the first subsystem, the thrust forces vector ρ_1 as a virtual input to the second subsystem and finally the last step is to design the control laws for the DC motor supply voltages u to stabilize the whole system. To reject the disturbance term d_1, a disturbance observer is designed to provide an estimate of d_1 which is then used in the second backstepping step. In addition, the second step will include an integrator to counteract the disturbance estimation error. As mentioned before, this multi-step design allows us to exploit the natural time scale separation between the TRMS dynamics and its actuator dynamics.

5.3. Disturbance observer-based controller

Based on the proposed control approach in Section 3, a disturbance observer-based backstepping controller is developed for the TRMS model formulated in Eq. (72). The controller equations are summarized as follows:

$$v_1 = \dot{x}_1^d - A_1 z_1,$$

Please cite this article as: R. Rashad, et al., A novel disturbance observer-based backstepping controller with command filtered compensation for a MIMO system, Journal of the Franklin Institute. (2016), http://dx.doi.org/10.1016/j.jfranklin.2016.07.017

$$\upsilon_2 = g_1^{-1}(-f_1 + \dot{\upsilon}_{1,f} + \Lambda_2\xi_2 - \hat{d}_1 + \overline{z}_1 + A_2 z_2),$$
$$u = g_2^{-1}[-f_2 + J_1^{-1}(\dot{\upsilon}_{2,f} + g_1^{\top}\overline{z}_2 + A_3 z_3)], \tag{77}$$

where $\upsilon_1, \upsilon_2 \in \mathbb{R}^2$ are virtual control signals and $A_1, A_2, A_3, \Lambda_2 \in \mathbb{R}^{2\times 2}$ are diagonal positive definite matrices. The term $\hat{d}_1 \in \mathbb{R}^2$ is the disturbance estimate generated using the disturbance observer depicted by

$$\hat{d}_1 = \delta_1 + \mu_1 x_2,$$
$$\dot{\delta}_1 = -\mu_1\delta_1 - \mu_1^2 x_2 - \mu_1(f_1 + g_1\upsilon_2), \tag{78}$$

where $\mu_1 > 0$ is the positive disturbance observer gain. The filtered command signals and their time derivatives are generated using the first order system

$$\dot{\upsilon}_{1,f} = \gamma(\upsilon_1 - \upsilon_{1,f}),$$
$$\dot{\upsilon}_{2,f} = \gamma(\upsilon_2 - \upsilon_{2,f}), \tag{79}$$

where $\gamma > 0$ is the command filter's cut-off frequency. Moreover, the term J_1 denotes the *Jacobian* matrix of ρ_1 such that

$$J_1(x_3) = \frac{\partial \rho_1}{\partial x_3} = \begin{bmatrix} \frac{dF_h}{dx_{31}} & 0 \\ 0 & \frac{dF_v}{dx_{32}} \end{bmatrix}. \tag{80}$$

The backstepping variables used in the control laws (77) include

$$z_1 = x_1^d - x_1, \quad z_2 = \upsilon_{1,f} - x_2, \quad z_3 = \upsilon_{2,f} - \rho_1,$$
$$\overline{z}_1 = z_1 - \varepsilon_1, \quad \overline{z}_2 = z_2 - \varepsilon_2, \quad \xi_2 = \int_0^t z_2(\tau)d\tau, \tag{81}$$

while the vectors $\varepsilon_1, \varepsilon_2 \in \mathbb{R}^2$ have the dynamics

$$\dot{\varepsilon}_1 = -A_1\varepsilon_1 + \upsilon_1 - \upsilon_{1,f} + \varepsilon_2,$$
$$\dot{\varepsilon}_2 = -A_2\varepsilon_2 - \Lambda_2\chi_2 + g_1(\upsilon_2 - \upsilon_{2,f}), \tag{82}$$

where $\chi_2 \in \mathbb{R}^2$ denotes the time integral of ε_2. Note that the functions f_1,f_2 satisfy Assumption 1, the functions g_1,g_2 satisfy Assumptions 1 and 2, and d_1 satisfies Assumption 4. Therefore, by the stability proof provided in Section 4.1, it is guaranteed that the output x_1 will track the desired trajectory x_1^d, from any initial conditions, within a guaranteed precision ϵ by using the DOB controller (77). The controller gains are designed based on the discussion presented in Section 3.4.

Remark 3. The determinants of g_1 and g_2 are given by

$$|det(g_1)| = \frac{l_m l_t |\cos x_{12}|}{J_v(|D\sin^2(x_{12}) + E\cos^2(x_{12}) + F|)} > 0, \quad for\ |x_{12}| < \frac{\pi}{2}$$
$$|det(g_2)| = \frac{1}{T_{tr}T_{mr}} > 0.$$

In the normal operation of the TRMS, the pitch angle x_{12} is physically constrained to be less than $\pi/2$. Thus, the functions g_1,g_2 satisfy Assumption 2.

Please cite this article as: R. Rashad, et al., A novel disturbance observer-based backstepping controller with command filtered compensation for a MIMO system, Journal of the Franklin Institute. (2016), http://dx.doi.org/10.1016/j.jfranklin.2016.07.017

6. Simulation results

The TRMS mathematical model (69) is used to build a MATLAB/Simulink® model to validate the proposed DOB controller and test its performance in the presence of disturbances. These disturbances applied to the system include the neglected dynamics (76) and external disturbances that may occur due to partial actuator failure. The purpose of the simulation studies is twofold. First, the simulation environment is used for tuning the controller gains and command filter's cut-off frequency. Moreover, it provides an indication of the characteristics of the control signals generated by the proposed controller. The results of two simulation scenarios will be presented in this section. The first scenario includes the stabilization of the yaw and pitch angles to zero starting from large initial conditions. In the middle of the scenario a 50 % loss of effectiveness (LoE) in the main rotor's thrust is simulated to resemble a partial actuator failure which may occur due to the propeller damage. The actuator LoE is simulated by multiplying the thrust force generated by the main rotor F_v by a scaling factor. The second simulation scenario includes tracking a sinusoidal trajectory for the yaw and pitch angles to test the convergence performance of the tracking error in the face of the disturbances due to the unmodeled dynamics. The simulation results for scenario 1 are presented in Fig. 2 while scenario 2 results are presented in Figs. 3–4.

For the first scenario, Fig. 2a shows that the yaw and pitch angles have successfully converged to zero starting from 60° and -30°, respectively. It can also be observed that the pitch angle recovered successfully in the presence of the severe 50% LoE introduced in the simulation at $t=30$ s. This performance has been achieved using the control action shown in Fig. 2b. The control inputs are observed to reach the saturation limit in the beginning due to the large initial conditions. However, once the errors have been decreased the yaw control input decreases to zero approximately, while the pitch control input reaches a constant value, in order to compensate the gravitational moment applied on the beam, which then changes to another level to compensate the actuator failure disturbance. Thus these results show the effectiveness of the proposed controller in rejecting disturbances.

The second scenario, as mentioned before, includes tracking a sinusoidal trajectory shown in Fig. 3a and b for the yaw and pitch angles respectively. The figures show that a very satisfactory tracking performance was achieved for the yaw angle while the pitch angle experienced repeated

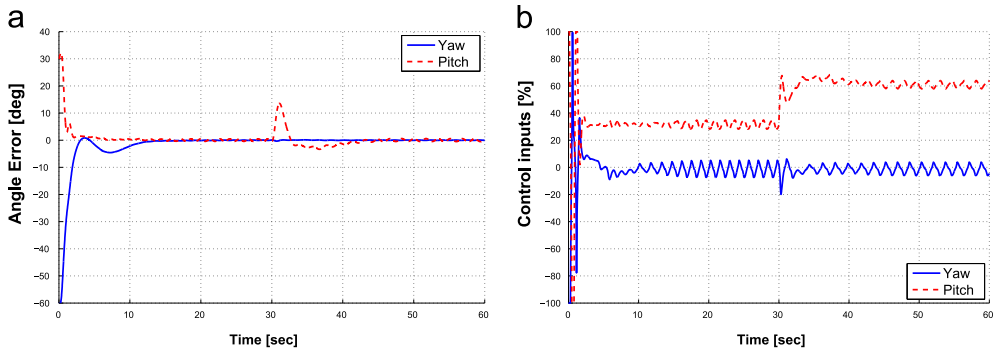

Angle errors Control signals

Fig. 2. Simulation scenario 1: Angle errors (left) and control signals (right) in the yaw (solid blue) and pitch (dashed red) axes. (a) Angle errors. (b) Control signals. (For interpretation of the references to color in this figure caption, the reader is referred to the web version of this paper.)

Please cite this article as: R. Rashad, et al., A novel disturbance observer-based backstepping controller with command filtered compensation for a MIMO system, Journal of the Franklin Institute. (2016), http://dx.doi.org/10.1016/j.jfranklin.2016.07.017

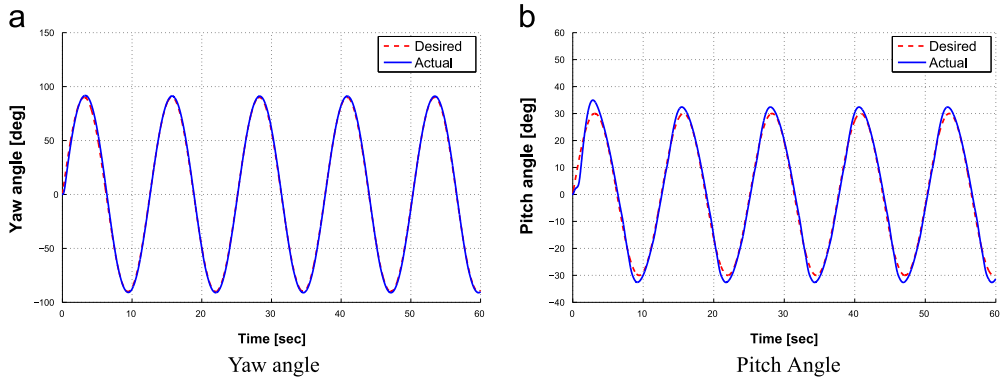

Fig. 3. Simulation scenario 2: Tracking performance of the yaw (left) and pitch (right) angles showing the desired (dashed red) and actual (solid blue) trajectories. (a) Yaw angle. (b) Pitch Angle. (For interpretation of the references to color in this figure caption, the reader is referred to the web version of this paper.)

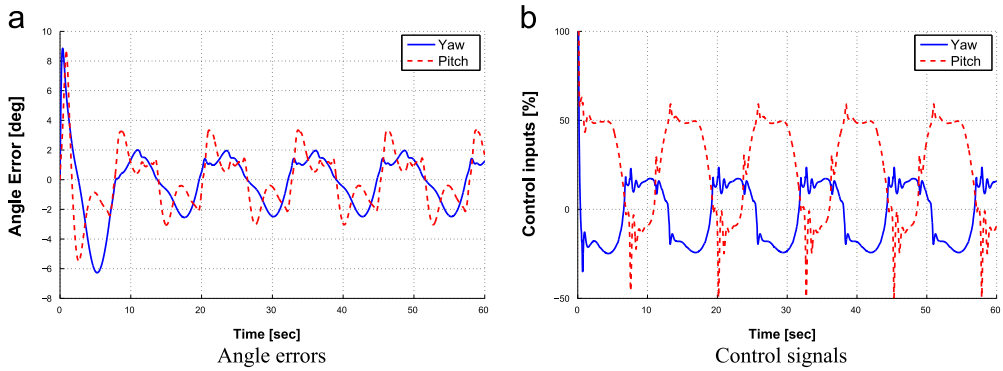

Fig. 4. Simulation scenario 2: Angle errors (left) and control signals (right) in the yaw (solid blue) and pitch (dashed red) axes. (a) Angle errors. (b) Control signals. (For interpretation of the references to color in this figure caption, the reader is referred to the web version of this paper.)

perturbations that occurred when the reference trajectory reaches a local minimum or maximum. This can be clearly observed in the tracking error plot shown in Fig. 4a. The reason for such performance is the time varying disturbances applied due to the cross-coupling dynamics (cf. *Eq.* (76)) on the pitch axis which causes a finite tracking error. Finally the control signals generated for the main and tail rotor can be found in Fig. 4b which shows a periodic behavior after some transients due to the initial zero velocity of the beam. The second scenario results prove the effectiveness of the tracking performance of the proposed control approach.

7. Experimental validation

The disturbance observer-based backstepping controller was implemented in hardware on the TRMS system shown in Fig. 5. In this system, we implemented the controller in real time using MATLAB/Simulink® in a PC computer. The control and data acquisition is performed using the equipped FPGA devices which operate in the Xilinx® technology. Similar to the simulation

Please cite this article as: R. Rashad, et al., A novel disturbance observer-based backstepping controller with command filtered compensation for a MIMO system, Journal of the Franklin Institute. (2016), http://dx.doi.org/10.1016/j.jfranklin.2016.07.017

Fig. 5. Experimental setup.

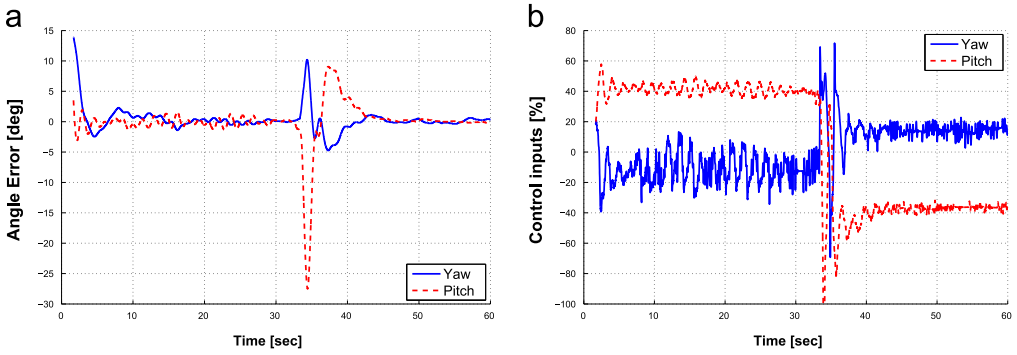

Angle errors Control signals

Fig. 6. Experiment 1: Angle errors (left) and control signals (right) in the yaw (solid blue) and pitch (dashed red) axes. (a) Angle errors. (b) Control signals. (For interpretation of the references to color in this figure caption, the reader is referred to the web version of this paper.)

studies carried out, two scenarios will be conducted for the experiments. The first scenario includes the stabilization of the yaw and pitch angles to zero starting from their equilibrium position. Due to the difficulty of implementing the partial actuator failure for the TRMS propellers in the lab, a constant load is attached to the pitch axis in the middle of the scenario instead. It was observed during the simulation studies conducted, that the effect on the system's response due to a constant disturbance applied to the pitch axis is equivalent to the effect of a constant partial actuator failure occurring in the main rotor. As for the second scenario includes tracking a sinusoidal trajectory for the yaw and pitch angles exactly similar to the simulation scenario discussed before. The experimental results for scenario 1 are presented in Fig. 6, while scenario 2 results are presented in Figs. 7–8. A common observation in all figures is that the

Please cite this article as: R. Rashad, et al., A novel disturbance observer-based backstepping controller with command filtered compensation for a MIMO system, Journal of the Franklin Institute. (2016), http://dx.doi.org/10.1016/j.jfranklin.2016.07.017

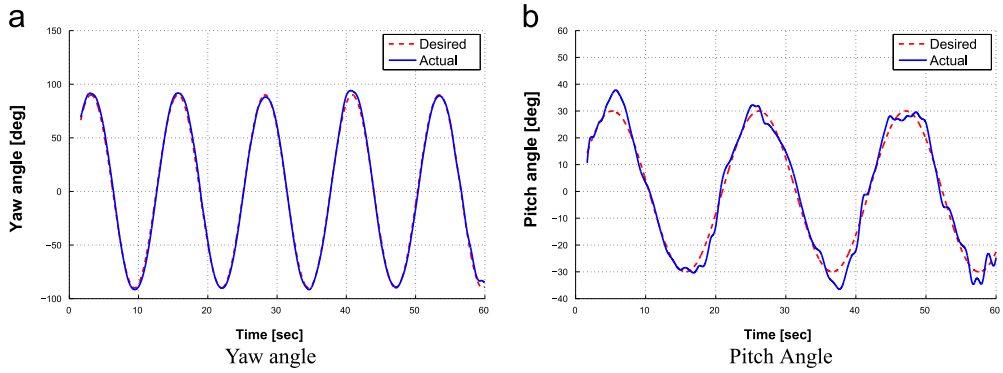

Fig. 7. Experiment 2: Tracking performance of the yaw (left) and pitch (right) angles showing the desired (dashed red) and actual (solid blue) trajectories. (a) Yaw angle. (b) Pitch Angle. (For interpretation of the references to color in this figure caption, the reader is referred to the web version of this paper.)

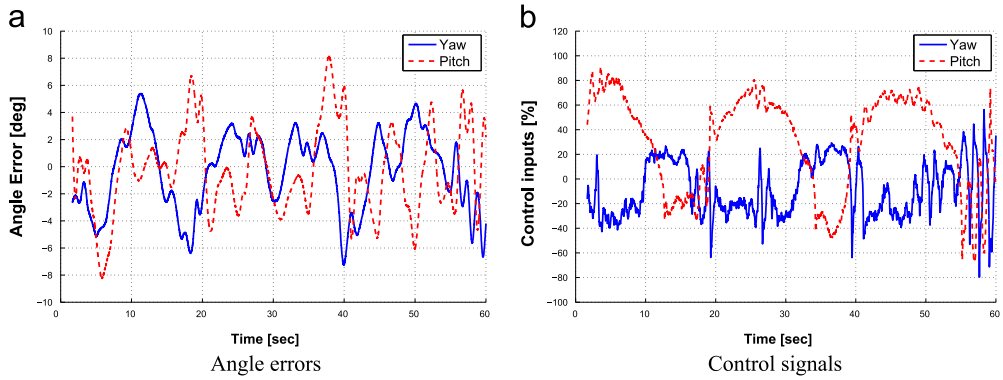

Fig. 8. Experiment 2: Angle errors (left) and control signals (right) in the yaw (solid blue) and pitch (dashed red) axes. (a) Angle errors. (b) Control signals. (For interpretation of the references to color in this figure caption, the reader is referred to the web version of this paper.)

signals are plotted after a small delay of 2 s, which is normal due to the operation of the setup's FPGA devices.

For the first scenario, the yaw and pitch angle errors successfully converged to zero both from the TRMS equilibrium configuration as shown in Fig. 6a. In addition, the pitch angle was stabilized by the controller after the constant load is attached to the pitch axis. The control signals of the tail and main DC motors are shown in Fig. 6b which show that after the load is added to the pitch axis, the control signals converged quickly to their new constant values to counteract the new disturbance.

As for the second scenario, it includes tracking the same sinusoidal trajectory as in the second simulation scenario as shown in Fig. 7a and b. The experimental results show that a satisfactory tracking performance was achieved for the yaw and pitch angles. As expected from the closed loop analysis of the system in Section 4, the tracking error is within a bounded limit due to the time-varying nature of the disturbances applied to the nominal model. This can be clearly shown in the tracking error plot in Fig. 8a. The reason why the performance of the pitch angle is more deteriorated than the yaw angle, is the regular disturbance applied on the vertical axis due to

Please cite this article as: R. Rashad, et al., A novel disturbance observer-based backstepping controller with command filtered compensation for a MIMO system, Journal of the Franklin Institute. (2016), http://dx.doi.org/10.1016/j.jfranklin.2016.07.017

gravitational effects not affecting the horizontal axis. Finally the control signals generated for the main and tail rotors are presented in Fig. 8b.

8. Conclusion

In this paper, a novel disturbance observer-based controller is proposed for the tracking control of a class of nonlinear MIMO systems. The proposed approach is based on the backstepping technique and is augmented with a disturbance observer to provide robustness to external disturbances applied on the system. Robustness is also provided against modeled dynamics intentionally neglected such that the system can be written in strict feedback form. The proposed approach includes as well the recently developed idea of command filtered backstepping. The analysis based on singular perturbation theory provides a proof of stability for this practical extension to the standard backstepping technique. To validate the effectiveness of the proposed control approach, it is implemented on the TRMS laboratory setup. Several simulation studies were performed and results showed that the controller stabilized the tracking errors to zero even in the presence of external disturbances and the unmodeled dynamics intentionally left out. Moreover, the proposed controller was implemented in hardware on a TRMS setup and the experimental results were similar to the simulation results which proves the robustness of the controller to model uncertainties and external disturbances applied.

References

[1] H.K. Khalil, Nonlinear Systems, 3rd ed., Prentice-Hall, 2002.
[2] T.I. Fossen, J.P. Strand, Tutorial on nonlinear backstepping: applications to ship control, Model. Ident. Control 20 (2) (1999) 83–134.
[3] R. Skjetne, T. Fossen, et al., On integral control in backstepping: Analysis of different techniques, in: Proceedings of the 2004 American Control Conference, vol. 2, IEEE, Boston, Massachusetts, USA, 2004, pp. 1899–1904.
[4] S. Li, J. Yang, W.-h. Chen, X. Chen, Disturbance Observer-Based Control: Methods and Applications, CRC Press, Boca Raton, Florida, USA, 2014.
[5] Z.-J. Yang, H. Tsubakihara, S. Kanae, K. Wada, C.-Y. Su, A novel robust nonlinear motion controller with disturbance observer, IEEE Trans. Control Syst. Technol. 16 (1) (2008) 137–147.
[6] T.-W. Hwang, M.-J. Tahk, Integrated backstepping design of missile guidance and control with robust disturbance observer, in: 2006 International Joint Conference, SICE-ICASE, IEEE, Busan, Korea (South), 2006, pp. 4911–4915.
[7] J.S. Bang, H. Shim, S.K. Park, J.H. Seo, Robust tracking and vibration suppression for a two-inertia system by combining backstepping approach with disturbance observer, IEEE Trans. Ind. Electron. 57 (9) (2010) 3197–3206.
[8] J. Farrell, M. Polycarpou, M. Sharma, W. Dong, et al., Command filtered backstepping, IEEE Trans. Autom. Control 54 (6) (2009) 1391–1395.
[9] R. Rashad, A. Aboudonia, A. El-Badawy, Backstepping trajectory tracking control of a quadrotor with disturbance rejection, in: Proceedings of the XXV International Conference on Information, Communication and Automation Technologies (ICAT), IEEE, Sarajevo, Bosnia and Herzegovina, 2015, pp. 1–7.
[10] C.-W. Tao, J.-S. Taur, Y.-H. Chang, C.-W. Chang, A novel fuzzy-sliding and fuzzy-integral-sliding controller for the twin-rotor multi-input–multi-output system, IEEE Trans. Fuzzy Syst. 18 (5) (2010) 893–905.
[11] J.-G. Juang, R.-W. Lin, W.-K. Liu, Comparison of classical control and intelligent control for a MIMO system, Appl. Math. Comput. 205 (2) (2008) 778–791.
[12] C.-S. Liu, L.-R. Chen, B.-Z. Li, S.-K. Chen, Z.-S. Zeng, Improvement of the twin rotor MIMO system tracking and transient response using fuzzy control technology, in: Proceedings of the 1st IEEE Conference on Industrial Electronics and Applications, IEEE, Singapore, 2006, pp. 1–6.
[13] C.-W. Tao, J.-S. Taur, Y. Chen, Design of a parallel distributed fuzzy lqr controller for the twin rotor multi-input multi-output system, Fuzzy Set Syst. 161 (15) (2010) 2081–2103.
[14] J.-G. Juang, W.-K. Liu, R.-W. Lin, A hybrid intelligent controller for a twin rotor MIMO system and its hardware implementation, ISA Trans. 50 (4) (2011) 609–619.

Please cite this article as: R. Rashad, et al., A novel disturbance observer-based backstepping controller with command filtered compensation for a MIMO system, Journal of the Franklin Institute. (2016), http://dx.doi.org/10.1016/j.jfranklin.2016.07.017

[15] S. Mondal, C. Mahanta, Second order sliding mode controller for twin rotor MIMO system, in: Proceedings of the Annual IEEE India Conference, IEEE, Hyderabad, India, 2011, pp. 1–5.
[16] S. Mondal, C. Mahanta, Adaptive second-order sliding mode controller for a twin rotor multi-input-multi-output system, IET Control Theory A 6 (14) (2012) 2157–2167.
[17] Inteco corporation, two rotor aerodynamical system user manual, Available at ⟨www.inteco.com.pl⟩, Krakow, Poland, 2011.
[18] W.-H. Chen, D.J. Ballance, P.J. Gawthrop, J. O'Reilly, A nonlinear disturbance observer for robotic manipulators, IEEE Trans. Ind. Electron. 47 (4) (2000) 932–938.
[19] C.-T. Chen, Linear System Theory and Design, Oxford University Press, Inc., New York, USA, 1995.
[20] P. Kokotovic, H.K. Khalil, J. O'reilly, Singular Perturbation Methods in Control: Analysis and Design, 25, SIAM, Philadelphia, USA, 1999.
[21] P. Wen, T.-W. Lu, Decoupling control of a twin rotor MIMO system using robust deadbeat control technique, IET Control Theory A 2 (11) (2008) 999–1007.
[22] P. Chalupa, J. Přikryl, J. Novák, Modelling of twin rotor MIMO system, Procedia Eng. 100 (2015) 249–258.
[23] Feedback corporation, twin rotor MIMO system 33–220 user manual (1998).

Please cite this article as: R. Rashad, et al., A novel disturbance observer-based backstepping controller with command filtered compensation for a MIMO system, Journal of the Franklin Institute. (2016), http://dx.doi.org/10.1016/j.jfranklin.2016.07.017